Rapid Communications

Signature for non-Stoner ferromagnetism in the van der Waals ferromagnet Fe_3GeTe_2

X. Xu,[1,*] Y. W. Li,[2,*] S. R. Duan,[1] S. L. Zhang,[3] Y. J. Chen,[1] L. Kang,[1] A. J. Liang,[3,4] C. Chen,[3,4] W. Xia,[3] Y. Xu,[1,5,6] P. Malinowski,[7] X. D. Xu,[7,8] J.-H. Chu,[7] G. Li,[3] Y. F. Guo,[3] Z. K. Liu,[3] L. X. Yang,[1,5,†] and Y. L. Chen[1,2,3,‡]

[1]*State Key Laboratory of Low Dimensional Quantum Physics, Department of Physics, Tsinghua University, Beijing 100084, China*

[2]*Department of Physics, Clarendon Laboratory, University of Oxford, Parks Road, Oxford OX1 3PU, United Kingdom*

[3]*School of Physical Science and Technology, ShanghaiTech University and CAS-Shanghai Science Research Center, Shanghai 201210, China*

[4]*Advanced Light Source, Lawrence Berkeley National Laboratory, Berkeley, California 94720, USA*

[5]*Frontier Science Center for Quantum Information, Beijing 100084, China*

[6]*RIKEN Center for Emergent Matter Science (CEMS), Wako, Saitama 351-0198, Japan*

[7]*Department of Physics, University of Washington, Seattle, Washington 98105, USA*

[8]*Department of Materials Science and Engineering, University of Washington, Seattle, Washington 98105, USA*

(Received 19 April 2019; revised manuscript received 27 February 2020; accepted 21 April 2020; published 11 May 2020)

The van der Waals ferromagnet Fe_3GeTe_2 has attracted great research attention recently due to its extraordinary properties. Here, using high-resolution angle-resolved photoemission spectroscopy, we systematically investigate the temperature evolution of the electronic structure of bulk Fe_3GeTe_2. We observe largely dispersive energy bands with exchange splitting that are in overall agreement with our density-functional theory calculation. Interestingly, the band dispersions barely change upon heating towards the ferromagnetic transition near 225 K, except for the reduction of quasiparticle coherence, which strongly deviates from the itinerant Stoner model. We suggest that the local magnetic moments may play a crucial role in the ferromagnetic ordering and the electronic structure of Fe_3GeTe_2, which will shed light on the generic understanding of itinerant magnetism in correlated materials.

DOI: 10.1103/PhysRevB.101.201104

Magnetism is not only a fascinating quantum phenomenon, but also immensely influences various emergent properties such as unconventional superconductivity [1–3], heavy fermion systems [4,5], topological quantum physics [6,7], and quantum critical behaviors [8,9]. In order to properly describe the magnetism in electronic materials, two paradigmatic frameworks have been established, concentrating on two opposing extremes: itinerant and local-moment magnetism [10]. Within the weak-coupling itinerant picture as represented by the well-known Stoner model, the spin-polarized exchange splitting of electron bands drives the long-range magnetic ordering in metallic systems, while the local magnetic moments take charge of the magnetism mainly in insulating materials according to the localized Heisenberg model. However, to distinguish these two mechanisms is usually challenging, especially in correlated materials, where the local magnetic moments, although screened by itinerant electrons, strongly modify the quasiparticle energy bands [11]. Such competition between local and itinerant magnetism has been well demonstrated by the longstanding debate regarding the nature of magnetic ordering in the cuprate and iron-based superconductors [3,12–15].

Recently, Fe_3GeTe_2, as a representative van der Waals ferromagnet, has been intensively studied due to the realization of tunable room-temperature ferromagnetism in its thin films [16,17]. Besides, bulk Fe_3GeTe_2 also exhibits fertile and intriguing properties, such as an extremely large anomalous Hall effect induced by topological nodal lines [18], Kondo lattice physics [19], a strongly enhanced electron mass [20], and a magnetocaloric effect [21]. Although it is widely believed that the ferromagnetism in Fe_3GeTe_2 is itinerant in nature [22], a local Heisenberg model can likewise properly describe the ferromagnetic ordering in Fe_3GeTe_2 [17]. There is even a debate regarding whether Fe atoms align ferromagnetically or antiferromagnetically in Fe_3GeTe_2 [23]. These intriguing yet mysterious properties allude to the possible effect of local moments in the ferromagnetism of Fe_3GeTe_2. Therefore, Fe_3GeTe_2 provides a rare platform to investigate the interplay between the ferromagnetism, electronic structure, and correlation effects. It will be elucidative to investigate the electronic structure of Fe_3GeTe_2, which is not yet adequate enough.

In this Rapid Communication, we systematically investigate the electronic structure of bulk Fe_3GeTe_2 and its temperature evolution using high-resolution angle-resolved photoemission spectroscopy (ARPES) and an *ab initio* band-structure calculation. The measured band structure in the ferromagnetic state is in overall agreement with our density-functional theory (DFT) calculation after renormalized by a

*These authors contributed equally to this work.
†lxyang@tsinghua.edu.cn
‡yulin.chen@physics.ox.ac.uk

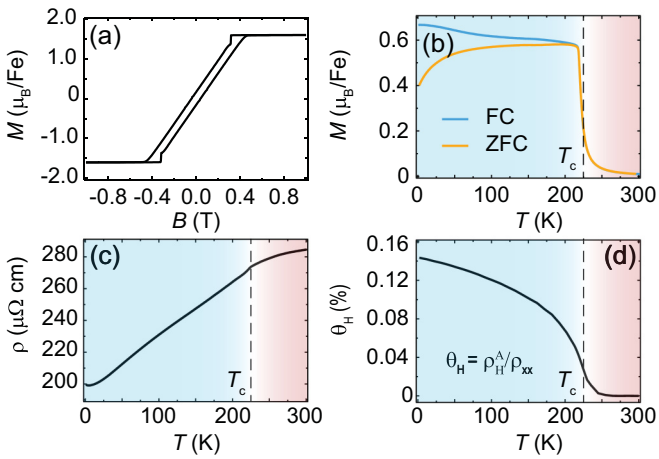

FIG. 1. (a) Magnetic moment as a function of magnetic field for Fe_3GeTe_2 measured at 2 K showing the magnetic hysteresis loop. (b) Temperature-dependent magnetization of Fe_3GeTe_2 measured under zero-field-cooling (ZFC) and field-cooling (FC) conditions. (c) Temperature-dependent resistivity of Fe_3GeTe_2. (d) Temperature-dependent anomalous Hall angle of Fe_3GeTe_2. All the data were collected with the magnetic field applied along the c axis. The vertical dashed line indicates the Curie temperature (T_c).

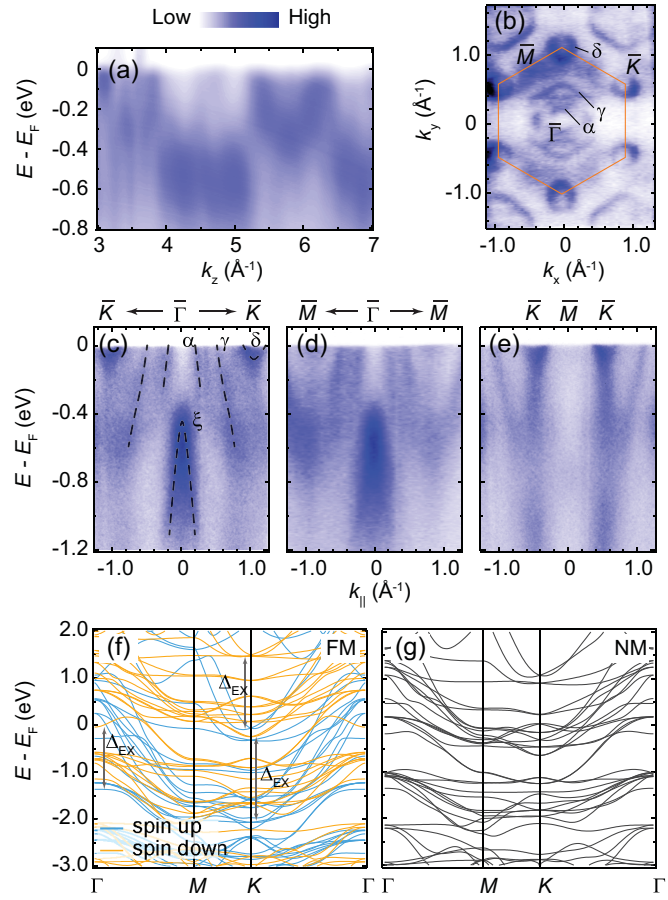

FIG. 2. (a) Band structure along $\bar{\Gamma}\bar{A}$ showing strong k_z dispersion in Fe_3GeTe_2 measured using photons ranging from 20 to 180 eV. (b) Fermi-surface map obtained by integrating ARPES intensity in an energy window of 20 meV near the Fermi energy (E_F). (c)–(e) Band dispersion along different high-symmetry directions. The black dashed curves are guides to the eyes for the band dispersions. (f), (g) DFT calculation of the band dispersions in ferromagnetic (FM) and nonmagnetic (NM) states. Data in (a) and (b)–(e) were collected using 114 eV photons with linearly (a) horizontal and (b)–(e) vertical polarizations.

factor of 1.6. Interestingly, upon heating towards the Curie temperature (T_c), we observe a minor change of the shape and position of the band dispersions, which is beyond the expectation of the itinerant Stoner model. Therefore, we argue that the local magnetic moments are crucial in the ferromagnetism and the electronic structure of Fe_3GeTe_2, although it is a prototypical itinerant ferromagnet. Our results provide important insights into not only the nature of ferromagnetism and other properties of Fe_3GeTe_2, but also a generic understanding of itinerant magnetism in correlated materials.

High-quality Fe_3GeTe_2 single crystals of size of $5 \times 5 \times 0.1\,mm^3$ were synthesized by a chemical transport method with iodine as the transport agent [16]. ARPES data were taken with various photon energies at beamline I05 of the Diamond Light Source (DLS) under proposal No. SI20683-1, beamline 9A of the Hiroshima Synchrotron Radiation Center (HSRC), and beamline 5-2 of the Stanford Synchrotron Radiation Laboratory (SSRL). Scienta R4000 electron analyzers are equipped at all three beamlines. The overall energy and angular resolutions are 15 meV and 0.3°. The electronic structures of bulk Fe_3GeTe_2 were calculated using DFT with the projected augmented-wave method as implemented in the Vienna *ab initio* simulation package [24,25]. The exchange correlation was considered in the Perdew-Burke-Ernzerhof (PBE) approximation [26]. The cutoff energy for the plane-wave basis was 400 eV and the reciprocal space integrations were calculated by summing in a Γ-centered $12 \times 12 \times 3$ mesh. The convergence of the mesh has also been checked in our calculations. Experimental lattice parameters were used with relaxations performed until the Feynman-Hellman force on each atom was smaller than 0.001 eV/Å. The atomic structure was further optimized by applying a van der Waals (vdW) correction with the DFT-D3 method of Grimme [27].

Fe_3GeTe_2 crystallizes into a layered hexagonal structure with the space group of $P63/mmc$ (No. 194). In the ferromagnetic state, the magnetic moments of all the Fe atoms align along the c axis below 225 K [21–23]. Figure 1 shows the magnetic transport measurements on Fe_3GeTe_2 with a field applied along the c axis. We observe a clear magnetic hysteresis loop showing the ferromagnetic nature of Fe_3GeTe_2. The magnetic moment saturates to a value of about $1.6\mu_B$/Fe above 0.4 T [Fig. 1(a)]. Figure 1(b) shows the temperature dependence of the magnetization. The T_c of Fe_3GeTe_2 is determined to be about 225 K, at which the temperature-dependent resistivity shows an anomaly [Fig. 1(c)], in consistence with previous measurements [20–22,28]. Below T_c, Fe_3GeTe_2 exhibits a large anomalous Hall effect, as shown by the temperature-dependent anomalous Hall angle in Fig. 1(d), which has been attributed to the topological nodal lines in the system [18].

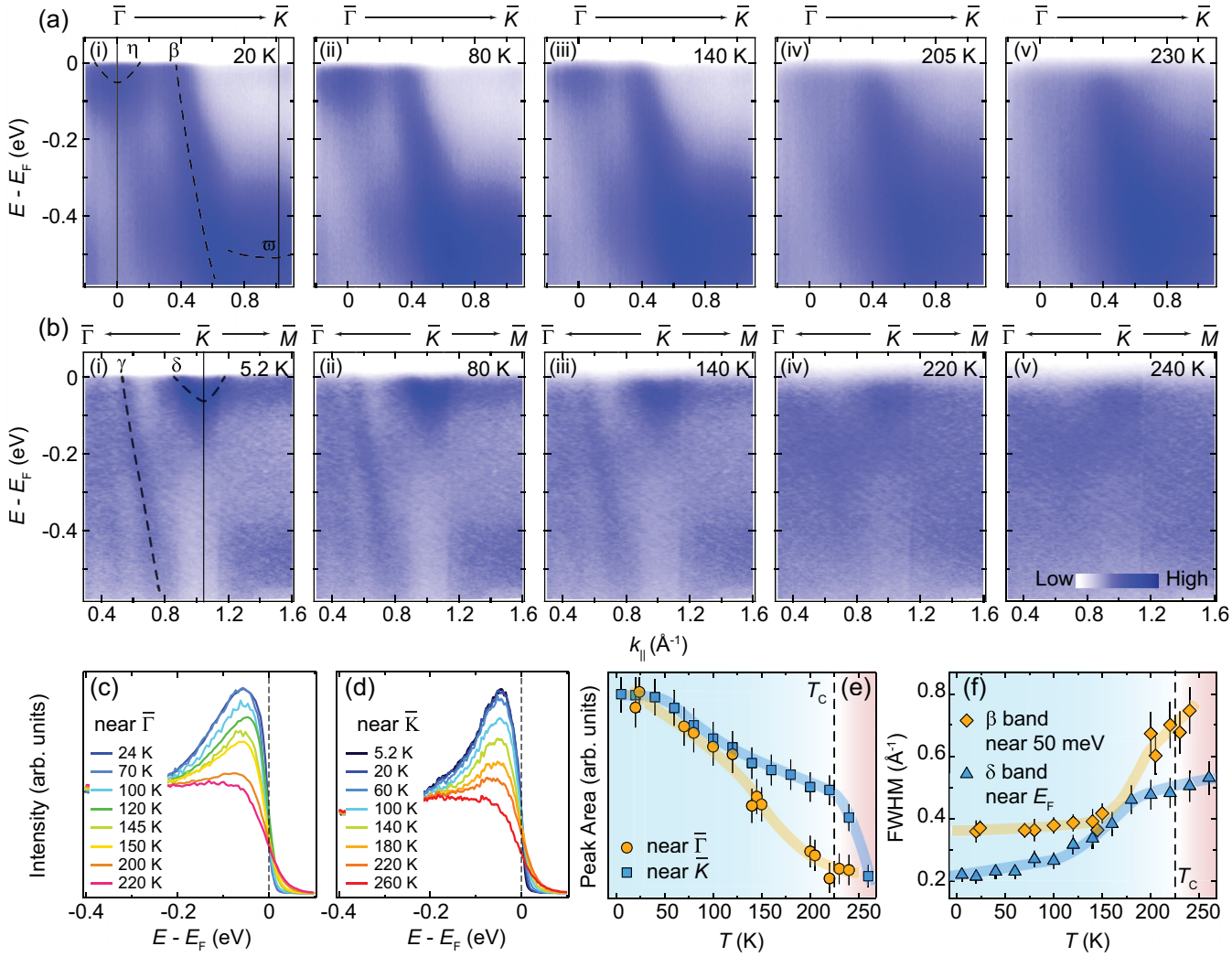

FIG. 3. (a), (b) Temperature evolution of the band dispersions near the (a) $\bar{\Gamma}$ and (b) $\bar{K}$ points. (c), (d) Energy distribution curves (EDCs) integrated in a momentum window of 0.25 $Å^{-1}$ near the (c) $\bar{\Gamma}$ and (d) $\bar{K}$ points. (e) The peak area of the EDCs in (c) and (d) as a function of temperature. EDC peak area is obtained by integrating the EDC in an energy window of 200 meV. (f) The full width at half maximum (FWHM) of the momentum distribution curves (MDCs) as a function of temperature. The MDCs are integrated in an energy window of 45 meV and fitted with a Lorentzian to extract its FWHM. The orange and blue curves are the guides to the eyes for the temperature evolution of the peak area and MDC width. Data in (a) and (b) were collected with photons at 27 and 114 eV, respectively.

Figure 2 investigates the electronic structure of Fe_3GeTe_2 in the ferromagnetic state at 10 K. Despite the weak interlayer coupling, we observe a strong k_z variation of the energy bands in Fig. 2(a) (see Supplemental Material [29]), suggesting strong interlayer coupling that can play an important role in the ferromagnetism of Fe_3GeTe_2 [17]. Figure 2(b) shows the Fermi surface in the k_x–k_y plane measured with 114 eV photons. We observe a hexagonal Fermi pocket near $\bar{\Gamma}$, with a complex texture structure inside. There is a small electron pocket near $\bar{K}$ and a distribution of blurred spectral weight near $\bar{M}$, in consistence with previous ARPES measurements and band-structure calculations [19]. Figures 2(c)–2(e) show the band dispersions along the high-symmetry directions. Due to the multiorbital nature and k_z dispersion of the energy bands, the measured Fermi surface and band dispersions strongly depend on the photon polarization and photon energy (see the Supplemental Material [29]). Using 114 eV photons with linearly vertical polarization, we observe mainly four bands in an energy range of 1.2 eV below the Fermi energy (E_F). The α and γ bands contribute to the hole pockets near $\bar{\Gamma}$, while the δ band contributes to the small electron pocket near $\bar{K}$. Our DFT calculation in Fig. 2(f) suggests that the calculated bands need to be renormalized by a factor of about 1.6 in order to obtain an overall agreement with the experiment (see Supplemental Material [29]). After renormalization, our calculation is consistent with previous dynamical mean-field theory (DMFT) calculations that suggest a relatively large Hubbard interaction in Fe sites and confirm the importance of electron correlation in the ferromagnetism of Fe_3GeTe_2 [18,20]. By comparing the calculated and measured δ band, we obtain an electron effective mass enhancement by a factor of about 1.6 (see Supplemental Material [29]), and we do not observe mass enhancement more significant than this value from the Fermi velocity of other bands. This value is much smaller

than that obtained from the Sommerfeld coefficient, which remains mysterious [20,22]. The calculated band structure in the ferromagnetic state shows a large exchange splitting [$\sim$1.5 eV as indicated by the arrows in Fig. 2(f)] compared with the nonmagnetic state [Fig. 2(g)], which is believed to drive the ferromagnetic ordering in Fe_3GeTe_2 according to the Stoner mechanism [22].

In order to unveil the nature of the ferromagnetism in Fe_3GeTe_2, we track the temperature evolution of its electronic structure in Fig. 3. Figures 3(a) and 3(b) show the band dispersions around $\bar{\Gamma}$ and $\bar{K}$ at selected temperatures measured with 27 eV (horizontally polarized) and 114 eV (vertically polarized) photons, respectively. We observe different bands η and β near $\bar{\Gamma}$ due to the k_z dispersion and polarization dependence of the energy bands (see Supplemental Material [29]). Both the η and δ bands only slightly shift towards lower binding energies with a spectral weight strongly suppressed at high temperatures. Figures 3(c) and 3(d) show the temperature evolution of the energy distribution curves (EDCs) near $\bar{\Gamma}$ and $\bar{K}$, respectively. The EDC peak intensity quickly decreases with increased temperature, as presented in Fig. 3(e). In addition, the ARPES spectra are strongly broadened upon warming towards T_c, suggesting a dramatic enhancement of the disordering level in the system, as estimated by the quickly increased momentum distribution curve (MDC) width in Fig. 3(f), which will scatter the coherent electron states near E_F into incoherent states and suppress the intensity near E_F. Both the suppression of the quasiparticle spectral weight and the increase of MDC width show an anomaly near T_c, suggesting an intimate correlation between the broadening of the spectra with the magnetism in the system. Thus, we speculate that the enhanced magnetic fluctuation with increased temperature [22] dominates the observed spectra broadening, although other effects such as the electron-phonon interaction may also contribute to the broadening. Notably, we observe the broadening of the energy bands in a large energy range, which is out of the expectation of itinerant spin fluctuations that mainly affect the states near E_F.

Within the Stoner model, a prototypical itinerant ferromagnet is expected to exhibit a temperature-dependent exchange splitting that disappears above T_c [Figs. 2(f) and 2(g)]. However, we do not observe a considerable change in the electronic structure with temperature in Fig. 3, as further tracked by MDCs and EDCs in Figs. 4(a) and 4(b). We quantify the band shift ΔE by tracking the temperature evolution of either EDC or MDC peaks ($\Delta E = \Delta k\, dE/dk$, where Δk is the MDC peak shift and dE/dk is the dispersion slope) and summarize the result in Fig. 4(c). We also compare the band shift with the temperature-dependent exchange splitting estimated from the magnetic moment that is scaled to half of the DFT calculated exchange splitting (about 1 eV taking the band renormalization into account). In a temperature range as large as 220 K, we observe a minuscule band shift (about 10% of the exchange splitting), which strongly deviates from the expectation within the itinerant Stoner model [Fig. 4(c); also see Supplemental Material [29]]. On the contrary, our observation fits better to the temperature-independent model based on the localized exchange interaction as indicated by the horizontal dashed line in Fig. 4(c) [30]. Clearly, a completely itinerant mechanism is not capable of explaining our experiment. The local magnetic moment, on the other hand, should be taken into account in order to properly describe the ferromagnetism in Fe_3GeTe_2. Our conclusion is supported by the observation of Kondo lattice behavior and the explanation of the ferromagnetism in Fe_3GeTe_2 within the Heisenberg model [17,19].

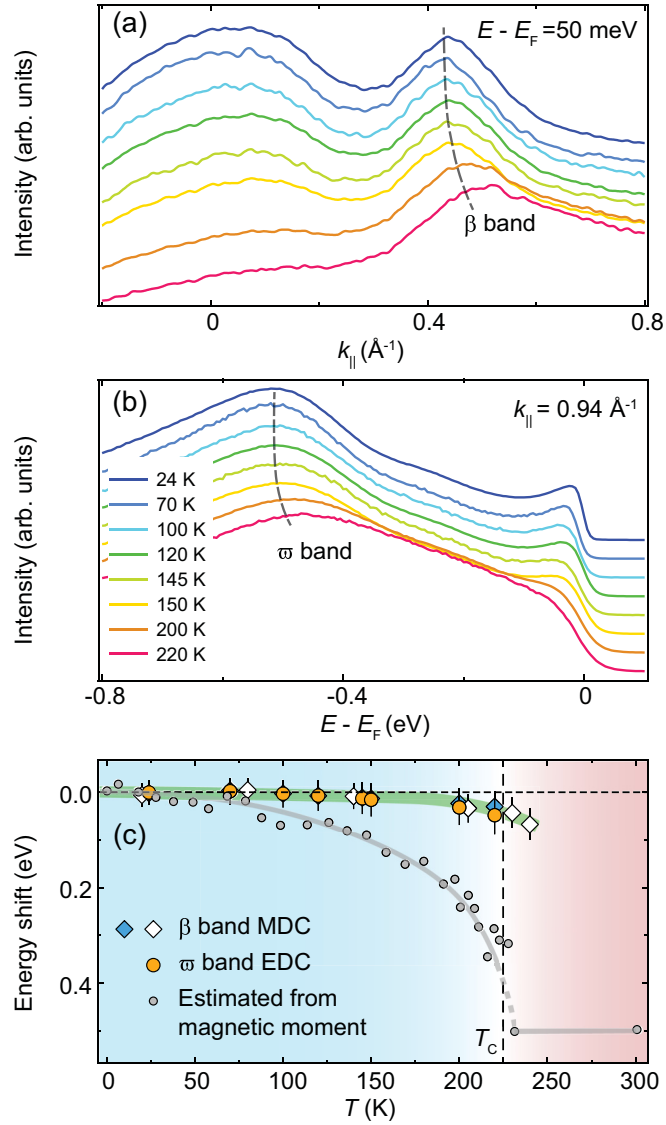

FIG. 4. (a) MDCs integrated in an energy window of 50 meV near -50 meV at selected temperatures. (b) EDCs integrated in a momentum window of 0.15 Å^{-1} near 0.94 sÅ^{-1} at selected temperatures. The gray dashed curves in (a) and (b) are guides to the eyes for the shift of EDC and MDC peaks with temperature. (c) The shift of energy bands as extracted from MDCs and EDCs as a function of temperature. The gray circles are the energy shift estimated from the magnetic moments in Fe_3GeTe_2 measured with neutron scattering in Ref. [21]. The gray and green curves are guides to the eyes for the temperature dependence of the energy shift. The temperature-independent dashed line shows the expected temperature evolution of the energy shift within a local-moment ferromagnet.

Our results mimic the behaviors of other itinerant ferromagnets such as $SrRuO_3$, in which a strong mass

enhancement, electron decoherence, and the local character of ferromagnetism indicated by a minor band shift with temperature were observed [31]. However, the underlying microscopic interaction and the impact of local moments on the electronic structure are different in these two systems. The quasiparticle effective mass is strongly renormalized by an electron-boson interaction in $SrRuO_3$, as demonstrated by a kink structure in the band dispersion. On the contrary, we did not observe any kink structure in Fe_3GeTe_2 and the electron effective mass is only enhanced by a factor of 1.6 due to the electronic correlation effect (see Supplemental Material [29]), although the specific heat measurement alludes to a dramatic enhancement of the quasiparticle effective mass [20,22]. The electron-electron interaction is more important in the magnetism of Fe_3GeTe_2 [20] than in $SrRuO_3$, since the effective on-site Coulomb interaction between Fe 3*d* electrons is much stronger that between Ru 4*d* electrons. On the other hand, the persistent exchange splitting in Fe_3GeTe_2 above T_c also resembles the results in the canonical ferromagnets Fe and Ni. Although the exchange splitting in Fe and Ni shows a strong temperature dependence, it survives above T_c [30,32–34], which was attributed to the retained local magnetic moments after the loss of long-range ferromagnetic ordering [31]. Considering the dominant role of Fe 3*d* orbitals in the ferromagnetism of Fe_3GeTe_2, it is reasonable that the local magnetic moments play similar roles in Fe_3GeTe_2 and Fe.

In conclusion, we have presented a systematic temperature evolution of the electronic structure of the van der Waals ferromagnet Fe_3GeTe_2. We observe substantial electron decoherence in a large energy range and a minor band shift upon warming towards T_c, which are against a weak-coupling itinerant picture. We argue that the local magnetic moments should be taken into account in order to understand the ferromagnetic ordering in the prototypical itinerant ferromagnet Fe_3GeTe_2. Our results resemble the observations in other prototypical itinerant ferromagnetic systems, which will deepen our generic understanding of the magnetism in condensed materials.

We thank M. Arita, K. Shimada, M. Hashimoto, S. W. Jung, and C. Cacho for the experimental support. This work was supported by the National Natural Science Foundation of China (Grants No. 11774190, No. 11674229, and No. 11634009), the National Key R&D Program of China (Grants No. 2017YFA0304600 and 2017YFA0305400), and EPSRC Platform Grant (Grant No. EP/M020517/1). The work at the University of Washington was supported by NSF MRSEC at UW (DMR-1719797) and the Gordon and Betty Moore Foundation's EPiQS Initiative, Grant No. GBMF6759 to J.-H.C. Y.F.G. acknowledges the support from the Shanghai Pujiang Program (Grant No. 17PJ1406200). L.X.Y. acknowledges the support from Tsinghua University Initiative Scientific Research Program.

[1] X. Chen, P. Dai, T. Xiang, D. Feng, and F.-C. Zhang, Nat. Sci. Rev. **1**, 371 (2014).
[2] J. Paglione and R. L. Greene, Nat. Phys. **6**, 645 (2010).
[3] E. Dagotto, Rev. Mod. Phys. **66**, 763 (1994).
[4] G. R. Stewart, Rev. Mod. Phys. **56**, 755 (1984).
[5] *Magnetism in Heavy Fermions*, edited by H. B. Radousky, Series in Modern Condensed Matter Physics Vol. 11 (World Scientific, Singapore, 2000).
[6] X.-L. Qi and S.-C. Zhang, Rev. Mod. Phys. **83**, 1057 (2011).
[7] M. Z. Hasan and C. L. Kane, Rev. Mod. Phys. **82**, 3045 (2010).
[8] D. A. Sokolov, M. C. Aronson, W. Gannon, and Z. Fisk, Phys. Rev. Lett. **96**, 116404 (2006).
[9] H. Kadowaki, Y. Tabata, M. Sato, N. Aso, S. Raymond, and S. Kawarazaki, Phys. Rev. Lett. **96**, 016401 (2006).
[10] K. Yosida, Theory of Magnetism, *Springer Series in Solid State Sciences* (Springer, Berlin, 1998).
[11] S. Schmitt, N. Grewe, and T. Jabben, Phys. Rev. B **85**, 024404 (2012).
[12] M. Vojta, Nat. Phys. **5**, 623 (2009).
[13] G. Xu, G. D. Gu, M. Hücker, B. Fauqué, T. G. Perring, L. P. Regnault, and J. M. Tranquada, Nat. Phys. **5**, 642 (2009).
[14] J. Zhao, D. T. Adroja, D.-X. Yao, R. Bewley, S. Li, X. F. Wang, G. Wu, X. H. Chen, J. Hu, and P. Dai, Nat. Phys. **5**, 555 (2009).
[15] J. M. Allred, K. M. Taddei, D. E. Bugaris, M. J. Krogstad, S. H. Lapidus, D. Y. Chung, H. Claus, M. G. Kanatzidis, D. E. Brown, J. Kang, R. M. Fernandes, I. Eremin, S. Rosenkranz, O. Chmaissem, and R. Osborn, Nat. Phys. **12**, 493 (2016).
[16] Z. Fei, B. Huang, P. Malinowski, W. Wang, T. Song, J. Sanchez, W. Yao, D. Xiao, X. Zhu, A.F. May, W. Wu, D. H. Cobden, J.-H. Chu, and X. Xu, Nat. Mater. **17**, 778 (2018).
[17] Y. Deng, Y. Yu, Y. Song, J. Zhang, N. Z. Wang, Z. Sun, Y. Yi, Y. Z. Wu, S. Wu, J. Zhu, J. Wang, X. H. Chen, and Y. Zhang, Nature (London) **563**, 94 (2018).
[18] K. Kim, J. Seo, E. Lee, K. T. Ko, B. S. Kim, B. G. Jang, J. M. Ok, J. Lee, Y. J. Jo, W. Kang, J. H. Shim, C. Kim, H. W. Yeom, B. Il Min, B.-J. Yang, and J. S. Kim, Nat. Mater. **17**, 794 (2018).
[19] Y. Zhang, H. Lu, X. Zhu, S. Tan, W. Feng, Q. Liu, W. Zhang, Q. Chen, Y. Liu, X. Luo, D. Xie, L. Luo, Z. Zhang, and X. Lai, Sci. Adv. **4**, eaao6791 (2018).
[20] J.-X. Zhu, M. Janoschek, D. S. Chaves, J. C. Cezar, T. Durakiewicz, F. Ronning, Y. Sassa, M. Mansson, B. L. Scott, N. Wakeham, E. D. Bauer, and J. D. Thompson, Phys. Rev. B **93**, 144404 (2016).
[21] V. Y. Verchenko, A. A. Tsirlin, A. V. Sobolev, I. A. Presniakov, and A. V. Shevelkov, Inorg. Chem. **54**, 8598 (2015).
[22] B. Chen, J. Yang, H. Wang, M. Imai, H. Ohta, C. Michioka, K. Yoshimura, and M. Fang, J. Phys. Soc. Jpn. **82**, 124711 (2013).
[23] J. Y. Yi, H. L. Zhuang, Q. Zou, Z. M. Wu, G. X. Cao, S. W. Tang, S. A. Calder, P. R. C. Kent, D. Mandrus, and Z. Gai, 2D Mater. **4**, 011005 (2017).
[24] P. E. Blöchl, Phys. Rev. B **50**, 17953 (1994).
[25] J. P. Perdew, K. Burke, and M. Ernzerhof, Phys. Rev. Lett. **77**, 3865 (1996).
[26] G. Kresse and J. Furthmüller, Comput. Mater. Sci. **6**, 15 (1996).
[27] S. Grimme, J. Antony, S. Ehrlich, and H. Krieg, J. Chem. Phys. **132**, 154104 (2010).

[28] Y. Liu, V. N. Ivanovski, and C. Petrovic, Phys. Rev. B **96**, 144429 (2017).

[29] See Supplemental Material at http://link.aps.org/supplemental/10.1103/PhysRevB.101.201104 for (I) sample characterization, (II) comparison between measured and calculated energy bands, (III) k_z dispersion of Fe_3GeTe_2, (IV) polarization dependence of the energy bands, (V) extraction of the effective mass of the *d* band, and (VI) temperature dependence of other bands.

[30] D. E. Eastman, F. J. Himpsel, and J. A. Knapp, Phys. Rev. Lett. **40**, 1514 (1978).

[31] D. E. Shai, C. Adamo, D. W. Shen, C. M. Brooks, J.W. Harter, E. J. Monkman, B. Burganov, D. G. Schlom, and K. M. Shen, Phys. Rev. Lett. **110**, 087004 (2013).

[32] E. Kisker, K. Schröder, M. Campagna, and W. Gudat, Phys. Rev. Lett. **52**, 2285 (1984).

[33] T. J. Kreutz, T. Greber, P. Aebi, and J. Osterwalder, Phys. Rev. B **58**, 1300 (1998).

[34] P. Tengdin, W. You, C. Chen, X. Shi, D. Zusin, Y. Zhang, C. Gentry, A. Blonsky, M. Keller, P. M. Oppeneer, H. C. Kapteyn, Z. Tao, and M. M. Murnane, Sci. Adv. **4**, eaap9744 (2018).